Bull. Mater. Sci., Vol. 39, No. 7, December 2016, pp. 1709–1724. © Indian Academy of Sciences.
DOI 10.1007/s12034-016-1321-9

Synthesis, characterization and isotherm studies of new composite sorbents

E S ZAKARIA[1], I M ALI[1], M KHALIL[1,*], T Y MOHAMED[2] and A EL-TANTAWY[1]
[1]Atomic Energy Authority, Hot Labs Center, Cairo 13759, Egypt
[2]Faculty of Science, Chemistry Department, Benha University, Benha 13518, Egypt

MS received 23 November 2015; accepted 25 April 2016

Abstract. **With different methods, different molar ratios and different surfactants have been investigated to reach the optimum conditions for synthesized zirconium tungstate (Zr(IV)W). Zr(IV)W with different molar ratios of o-toluidine was synthesized to reach the optimum conditions for poly-o-toluidine zirconium tungstate (POTZr(IV)W). POTZr(IV)W with different molar ratios of tungstate was used to achieve the optimum conditions for poly-o-toluidine Zr(IV) tungstophosphate (POTZr(IV)WP). The Na^+ capacity for all the prepared materials was investigated in order to determine the best ion exchanger towards the absorbed ions. The chemical and physical properties of materials were determined. Sorption isotherm studies of La^{3+}, Ce^{3+}, Nd^{3+} and Sm^{3+} ions were performed at different reaction temperatures and analysed by Langmuir, Freundlich, Dubinin–Raduchkivich and Temkin isotherm models. Thermodynamic parameters such as $\Delta G°$, $\Delta H°$ and $\Delta S°$ were determined and found to be endothermic and spontaneous in nature.**

Keywords. **Ion exchanger; composite; synthesis; characterization; isotherm; lanthanides.**

1. Introduction

In the last decades, the demand for rare-earth elements (REEs) was increased due to the development of many advanced technologies. So REEs have received great attention due to their importance in different applications like electronics, catalysts, used in clean energy technologies of the future such as wind turbines, electric vehicles and phosphors. REEs are produced during the uranium fission and present in the radioactive waste [1]. REE-rich sources have rare-earth oxides (REOs), such as carbonate-based bastnasite and phosphate-based monazite. Lanthanide group elements are chemically similar, so their separations are difficult. Lanthanide separation and purification are important for controlling of radioactive wastes, renewable energy technologies of the future, mining industries as well as environmental remediation and pollution control. As a result of being fission product, REEs can be used as non-active simulators to investigate the expected behaviour of the long-lived, radiotoxic minor actinides [1].

Different technologies are applied for the purpose of separation and purification, such as chemical precipitation, coagulation, sedimentation, flotation, filtration, membrane processes, electrochemical techniques, ion exchange, biological processes and chemical reactions. One of the most promising technologies widely applied for metal ions retention is ion exchange. This technique has many advantages such as the simplicity of equipment, operation and regeneration [2]. In the early days, organic resins are introduced for remediation of waste waters that may contain toxic, radioactive or precise metal ions. These organic resins are preferably used in certain process such as water treatment due to their high ion exchange capacity (IEC), good mechanical properties, but they have limitations such as poor thermal, chemical and radioactive stability, they are able to swell and they have no selective behaviour for specific metal ions [3].

Due to the limitations of organic resins, researchers developed inorganic ion exchangers that have good chemical, thermal and radiation stability, selectivity for specific metal ions, but they have limitations like low capacity compared to organic resins and irreproducibility [4]. Most of the inorganic ion exchangers [5–7], such as lithium titanate, tin silicate, tin and titanium-ferrocyanides, etc., exhibit very low ion exchange efficiency in the high acidic media.

Many researchers take great attention to create a new class of hybrid organic–inorganic ion exchangers to combine the main advantages of each constituent [8]. These hybrid ion exchangers consist of inorganic ion exchangers and organic binding matrices. Composite ion exchangers are favourably used, as they have many advantages such as improved mechanical properties due to binding of organic polymer and its granulometric properties makes them more suitable for the application in column operations. Chemical inertness, high thermal and radiation stability, reproducibility and high selectivity make them able for direct conversion to stable crystalline phases from which radionuclides cannot be leached. This makes such materials suitable for direct disposition for the disposal of long-lived heat-producing

*Author for correspondence (magdykhalil7@yahoo.com)

radionuclides. In this study various samples of poly-o-toluidine zirconium tungstophosphate (POTZr(IV)WP) with different molar ratios were prepared to obtain the most effective sample, which was used for the retention of important metal ions such as La^{3+}, Ce^{3+}, Sm^{3+} and Nd^{3+} from aqueous solution. POTZr(IV)WP composite material was characterized by FTIR, XRD, TG-DTA, XRF, SEM and CHN elemental analysis, chemical stability and pH titration curve. Effect of the resin dosage experiment was studied to determine the optimum V/m used in batch experiments. Sorption isotherm studies were conducted in order to investigate the sorption mechanism controlling the sorption process of La^{3+}, Ce^{3+}, Sm^{3+} and Nd^{3+} onto POTZr(IV)WP.

2. Material and method

2.1 *Chemicals and reagents*

The main reagents used for the synthesis were zirconium oxychloride ($ZrOCl_2 \cdot 8H_2O$), N-cetyl-N,N,N, trimethyl ammonium bromide, CTAB ($C_{19}H_{42}BrN$), sodium dodecyl sulphate, SDS ($CH_3(CH_2)_{11}OSO_3Na$), all obtained from EL NASR Pharmaceutical Chemicals Co., Egypt. Sodium dioctyl sulphosuccinate, SDSC ($C_{20}H_{37}NaO_7S$), was obtained from KAMSONS Chemicals Pvt. Ltd, India. Potassium persulphate ($K_2S_2O_8$) was obtained from LOBA CHMIE, India. Sodium tungstate ($Na_2WO_4 \cdot 2H_2O$), ortho-toluidine ($C_{14}H_{18}Cl_2N_2$), nitric acid, acetic acid, ortho-phosphoric acid and hydrochloric acid were purchased from Adwic, Egypt. Neodymium (III) nitrate hexahydrate was purchased from FLUKA. Samarium (III) chloride hexahydrate was purchased from Strem Chemicals, United States. Cerium (III) nitrate hexahydrate was purchased from Merch, Germany. Lanthanum (III) chloride hexahydrate was purchased from Winlab. All other reagents and chemicals were of analytical grade purity.

2.2 *Preparation of the reagent solutions*

Various concentrations of zirconium oxychloride, sodium tungstate and ortho-phosphoric acid solutions were prepared in bi-distilled water, while the solutions of o-toluidine (0.28 M) and potassium persulphate (0.1 M) were prepared in 1 M HCl solution.

2.3 *Synthesis of adsorbent materials*

Various adsorbents were synthesized as poly-o-toluidine, zirconium tungstate (Zr(IV)W) zirconium tungstophosphate and poly-o-toluidine zirconium tungstophosphate with different methods.

2.3a *Synthesis of poly-o-toluidine* A polymer of o-toluidine gels was prepared by mixing an equal volume ratio of the solution of 0.1 M potassium persulphate and 0.14 M o-toluidine. The solution of potassium persulphate was added drop by drop in the flask containing o-toluidine with continuous stirring at the room temperature. Potassium persulphate acted as an oxidizing agent resulting in the formation of polymer gel, which was kept for 1 h at room temperature [9].

2.3b *Synthesis of Zr(IV)W with hydrothermal method* Hydrothermal technique was used for the preparation of zirconium tungstate. A quantity of 200 ml (0.1 M) sodium tungstate solution was added drop wise to 200 ml (0.1 M) zirconium oxychloride solution and 0.2 g CTAB with continuous stirring by magnetic stirrer at room temperature (25 ± 1°C). The pH of the mixture was adjusted at 1.5 by adding an aqueous solution of ammonia or nitric acid with constant stirring. Then, the white coloured gel was transferred into a Teflon-lined stainless-steel autoclave (400 ml) to carry out hydrothermal reactions at 150°C for 24 h. After the autoclave was allowed to cool at room temperature naturally, the supernatant liquid was decanted and the gel was rewashed with bi-distilled water in order to remove fine adherent particles and then filtered by using a centrifugation (about 4000 rpm). The excess acid was removed by washing with bi-distilled water and the material was dried in an air oven at 60 ± 1°C. The dried product was immersed in bi-distilled water to obtain small granules. The material was converted to H^+ form by treating with 0.1 M HNO_3 for 24 h with occasional shaking intermittently replacing the supernatant liquid with fresh acid. The excess acid was removed after several washings with bi-distilled water and then dried at 60 ± 1°C. Several particles size of material was obtained by sieving and kept for further usage in the batch experiments [10].

2.3c *Synthesis of Zr(IV)W with sol–gel method* Various samples of inorganic precipitate of Zr(IV) tungstate was prepared at room temperature based on using different surfactants (CTAB, SDS and SDSC). The solution of 0.1 M sodium tungstate to a mixture of aqueous solution of 0.1 M zirconium oxychloride and (0.1 g of CTAB, 0.5 g of SDS and 1 ml of SDSC) with continuous stirring by magnetic stirrer at (25 ± 1°C). Then the pH of the obtained mixture was adjusted at 1.5 by adding an aqueous solution of ammonia or nitric acid with constant stirring. Zirconium tungstate was obtained as white coloured gel.

2.3d *Synthesis of zirconium tungstophosphate (Zr(IV)WP)* Zirconium tungstophosphate inorganic ion exchanger was prepared by adding a mixture containing aqueous solution of 0.1 M sodium tungstate and 4 M H_3PO_4 gradually to a mixture containing aqueous solution of 0.1 M zirconium oxychloride and 0.1 g of cetyl trimethyl ammonium bromide with continuous stirring by magnetic stirrer at (25 ± 1°C). The pH of the mixture was adjusted at 1.5 by adding an aqueous solution of ammonia or nitric acid with constant

stirring. Then white coloured gel was obtained as zirconium tungstophosphate [11].

2.3.e *Synthesis of poly-o-toluidine zirconiumtungstate (POTZr(IV)W)* Poly-o-toluidine Zr(IV) tungstate cation exchanger was prepared by sol–gel method through different mixing ways.

2.3.e1 *Synthesis of POTZr(IV)W by normal method* In this method, the organic polymer of o-toluidine was added to the inorganic precipitate of Zr(IV)W with constant stirring. The resultant mixture turned slowly into brownish green coloured slurries. The obtained solution pH was adjusted to 1.5 by ammonia solution or nitric acid. The obtained slurries were kept for 24 h at room temperature 25 ± 1°C for digestion, then as mentioned below [10].

2.3.e2 *Synthesis of POTZr(IV)W by chelation method* In this method the hybrid material was prepared by adding solution of 200 ml (0.1 M) sodium tungstate to the mixture solution of 100 ml (0.1 M) zirconium oxychloride, 0.1 g CTAB and 50 ml (0.05 M) o-toluidine, then adding 50 ml (0.1 M) $K_2S_2O_8$. The obtained mixture solution pH value was adjusted to 1.5 by adding ammonia solution or nitric acid. The obtained slurries were kept for 24 h at room temperature 25 ± 1°C for digestion, then as mentioned below.

2.3.e3 *Synthesis of POTZr(IV)W by insitue method* In this method the composite material was prepared by adding the mixture solution of 200 ml (0.1 M) sodium tungstate and 50 ml (0.1 M) $K_2S_2O_8$ drop wise to the mixture solution of 50 ml (0.05 M) o-toluidine and 100 ml (0.1 M) zirconium oxychloride with 0.1 g CTAB. The resultant mixture turned slowly into brownish green coloured slurries. The obtained solution pH was adjusted to 1.5 by ammonia solution or nitric acid and the obtained slurries were kept for 24 h at room temperature 25 ± 1°C for digestion. The supernatant liquid was decanted and the gel was rewashed with bi-distilled water in order to remove fine adherent particles, then filtered by using a centrifugation (about 4000 rpm). The excess acid was removed by washing with bi-distilled water and the material was dried in an air oven at 60 ± 1°C. The dried product was immersed in bi-distilled water to obtain small granules. The material was converted to H^+ form by treating with 0.1 M HNO_3 for 24 h with occasional shaking intermittently replacing the supernatant liquid with fresh acid. The excess acid was removed after several washings with bi-distilled water and then dried at 60 ± 1°C. Several particles size of material was obtained by sieving and kept for further usage in the batch experiments. In this way a number of samples of POTZr(IV)W were synthesized under variable conditions. The sodium ion exchange capacities were 0.16, 0.15 and 0.24 for the normal, chelation and insitue methods, respectively. On the basis of the highest IEC (0.24 meq g^{-1}), sample prepared by insitue method was selected for further preparation studies as in table 1.

2.3.f *Synthesis of poly-o-toluidine Zr(IV) tungstophosphate (POTZr(IV)WP)* POTZr(IV)WP was synthesized with different molar ratios to obtain the best sample. A volume of 0.05, 0.1, 0.15 and 0.28 M of o-toluidine was added

Table 1. Preparation conditions of various samples of POTZr(IV)WP hybrid cation exchange materials.

Samples	Mixing volume ratio (v/v)			Mixing volume ratio (v/v) of 0.05 M o-toluidine	Surfactants	Appearance after drying	Na^+ ion exchange capacity (meq g^{-1})
	$ZrOCl_2 \cdot 8H_2O$	$Na_2WO_4 \cdot 2H_2O$	H_3PO_4				
S-1	1 (0.1M)	1 (0.1M)	—	—	—	White granules	0.11
S-2	1 (0.1M)	1 (0.1M)	—	—	0.5 g CTAB	White granules	0.14
S-3	1 (0.1M)	1 (0.1M)	—	—	0.5 g SDS	White granules	0.12
S-4	1 (0.1M)	1 (0.1M)	—	—	1 ml SDSC	White granules	0.16
S-5	1 (0.1M)	1 (0.1M)	—	—	0.2 g CTAB (hydrothermal)	White granules	0.22
S-6	1 (0.1 M)	1 (0.1 M)	—	0.5	0.1 g CTAB	Black shiny	0.3
S-7	2 (0.1 M)	1 (0.1 M)	—	0.5	0.1 g CTAB	Black shiny	0.26
S-8	1 (0.1 M)	2 (0.1 M)	—	0.5	0.1 g CTAB	Black shiny	0.38
S-9	1 (0.1 M)	2 (0.2 M)	—	0.5	0.1 g CTAB	Black shiny	0.32
S-10	2 (0.2 M)	1 (0.1 M)	—	0.5	0.1 g CTAB	Black shiny	0.1
S-11	1 (0.2M)	2 (0.1M)	—	0.5	0.1 g CTAB	Black shiny	0.28
S-12	1 (0.1 M)	2 (0.1 M)	0.5 (1M)	0.5	0.1 g CTAB	Black shiny	0.44
S-13	1 (0.1 M)	2 (0.1 M)	0.5 (4M)	0.5	0.1 g CTAB	Black shiny	0.8
S-14	1 (0.1 M)	2 (0.1 M)	0.5 (8M)	0.5	0.1 g CTAB	Black shiny	0.92
S-15	1 (0.1 M)	2 (0.1 M)	0.5 (4M)	0.5 (0.1 M)	0.1 g CTAB	Black shiny	0.98
S-16	1 (0.1 M)	2 (0.1 M)	0.5 (4M)	0.5 (0.15 M)	0.1 g CTAB	Black shiny	1.32
S-17	1 (0.1 M)	2 (0.1 M)	0.5 (4M)	0.5 (0.28 M)	0.1 g CTAB	Black shiny	1.8
S-18	1 (0.1 M)	2 (0.1 M)	0.5 (4M)	0.5 (0.28 M)	0.2 g CTAB	Black shiny	1.3
S-19	1 (0.1 M)	2 (0.1 M)	0.5 (4M)	0.5 (0.28 M)	0.3 g CTAB	Black shiny	1.5

to the mixture solution of 0.1 M $ZrOCl_2 \cdot 8H_2O$ and 0.1 M $Na_2WO_4 \cdot 2H_2O$, then the obtained slurries were washed with bi-distilled water and dried at 60°C. Later the resulted slurries were immersed in HNO_3, washed again several times, dried and kept in a desiccator for further studies.

POTZr(IV)WP cation exchanger was prepared by sol–gel insitue method. The mixture solution of 200 ml (0.1 M) sodium tungstate, 50 ml (0.1 M) $K_2S_2O_8$ and 50 ml (4 M) H_3PO_4 was added drop wise to a mixture solution of 50 ml (0.05 M) o-toluidine and 100 ml (0.1 M) zirconium oxychloride with 0.1 g CTAB with constant stirring under the best conditions for the preparation of Zr(IV)W. The resultant mixture turned slowly into brownish green coloured slurries. The resultant slurries were kept for 24 h at room temperature 25 ± 1°C for digestion. The supernatant liquid was decanted and the gel was rewashed with bi-distilled water in order to remove fine adherent particles, then filtered by using a centrifugation (about 4000 rpm). The excess acid was removed by washing with bi-distilled water and the material was dried in an air oven at 60 ± 1°C. The dried product was immersed in bi-distilled water to obtain small granules. The material was converted to H^+ form by treating with 0.1 M HNO_3 for 24 h with occasional shaking intermittently replacing the supernatant liquid with fresh acid. The excess acid was removed after several washings with bi-distilled water and then dried at 60 ± 1°C. Several particles size of material was obtained by sieving and kept for further usage in the batch experiments [9]. In this way a number of samples of POTZr(IV)WP were synthesized under variable conditions (table 1). On the basis of the highest IEC (1.8 meq g^{-1}) together with physical stability and appearance of beads, sample S-17 was selected for detailed studies.

2.4 *Instruments and characterization of the prepared materials*

The Fourier transform infrared spectra were recorded using an FTIR spectrometer, using Nicolet iS10 spectrometer from Meslo, USA, in the range of 4000–400 cm^{-1} with 32 scans at a resolution of 2 cm^{-1} using KBr disc technique. The thermal stability of prepared compounds was ascertained by thermogravimetric analysis (TGA) and differential thermal analysis (DTA). Shimadzu DTA–TGA system of type DTA-TGA-60, Japan, with platinum crucible and alumina powder reference was used for the measurements of the phase changes and weight losses of the sample, respectively. Samples were heated up to a temperature of 1000°C in the presence of nitrogen atmosphere to avoid thermal oxidation of the powder sample with a heating rate of 20°C min^{-1}. Measurements of powder X-ray diffraction patterns were carried out using Shimadzu X-ray diffractometer, Model XD 490, Shimadzu, Japan, with a nickel filter and Cu-K_α radiation tube. Samples were very lightly ground and mounted on a flat sample plate at room temperature. The average crystal size of the powder was calculated from diffraction peak full-width at half-maximum (FWHM), using the Scherrer equation. Scanning electron microscopy (SEM) was performed using a high-resolution scanning electron microscope XL30 SFEG, Phillips, the Netherlands. The metal ion concentrations were measured using UV-Visible spectrophotometer, Shimadzu, Japan, and an inductively coupled plasma atomic emission spectroscopy, ICPs-7510, Shimadzu, Japan. All the pH values of different solutions were measured using pH a glass electrode, AD/030, Romania, with microprocessor and have an accuracy of ± 0.02 units. The pH metre scale was calibrated using two standard buffer solutions within the pH range of the measured solution before each experiment. The deviation in the readings was in the range of ± 0.01 at the laboratory temperature 25 ± 1°C. A thermostated shaker, Clifton, England, was used for ion exchange equilibrium experiments. All samples and chemicals used in this work were weighted using an analytical balance of ADAM, pw124, Germany, having maximum sensitivity of 120 g and accuracy ± 0.0001 g.

2.5 *Sodium IEC*

The ion exchange capacities of different prepared ion exchangers were determined by acid–base titration. The weighted samples of the ion exchanger in its H^+ form were soaked in 50 ml of 1 M NaCl solution for at least 12 h with shaking at ambient temperature to exchange protons with sodium ions. The ion exchanged solution was titrated to the phenolphthalein end point (2 drops of ph.ph indicator, 1% ph.ph in ethanol) with a NaOH solution of 0.1 M concentration. The sodium IEC was calculated using the following equation:

$$\text{IEC (meq g}^{-1}) = V_{\text{NaOH}} \frac{C_{\text{NaOH}}}{W_{\text{d}}}, \tag{1}$$

where V_{NaOH}, C_{NaOH} and W_{d} are the volume of NaOH consumed in titration, the concentration of NaOH solution and the weight of the dry sample, respectively.

2.6 *Chemical stability*

In order to measure the stability of composite against various media, the chemical stability of POTZr(IV)WP in various acids media (HCl and HNO_3), base (NaOH) and organic solvent (acetic acid) was studied by batch experiments. The chemical stability of Zr(IV)WP was determined only in acids media (HCl and HNO_3). A quantity of 50 mg portions of each of POTZr(IV)WP and Zr(IV)WP were contacted for 24 h at room temperature with 50 ml of a particular medium with intermittently shaking. After contact, the ion exchanger was separated, then dried at 70°C and the weight losses (%) were calculated.

2.7 *Effect of resin dosage*

In order to obtain the optimum batch factor (V/m) used for performing the experiments, different adsorbent masses

(0.025, 0.033, 0.05, 0.1, 0.2 and 0.4 g) of POTZr(IV)WP were conducted with 10 ml of 50 mg l^{-1} samarium(III) chloride solution in several stoppered glass bottles and kept in the thermostatic shaker water bath at room temperature for sufficient time to obtain the equilibrium. The supernatant solutions were analysed using UV-Visible spectrophotometer and the percent uptake was calculated as follows:

$$\%\ \text{Uptake} = \frac{C_0 - C_e}{C_0} \times 100, \tag{2}$$

where C_0 and C_e are the initial and equilibrium concentrations of metal ion in mg l^{-1}.

2.8 *pH titration*

The pH titration studies were performed by Topp and Pepper method to determine the functionality behaviour of POTZr(IV)WP [12,13]. Each 0.05 g of POTZr(IV)WP composite cation exchanger in H^+ form were placed in each of the several glass bottles containing equimolar solution of alkali metal chlorides and their corresponding hydroxide in different volume ratios such as NaCl–NaOH, LiCl–LiOH, KCl–KOH systems. The final volume was kept at 10 ml to maintain the ionic strength constant with intermittent shaking. The pH of the solution was recorded after every 24 h till the equilibrium was attained. The pH of the solution was determined after attaining the equilibrium (which needed about 7 days) and the pH was plotted against the milliequivalents of OH^- ions that were added.

2.9 *Sorption isotherm studies*

Sorption process of the studied metal ions (La^{3+}, Ce^{3+}, Nd^{3+} and Sm^{3+}) onto POTZr(IV)WP was carried out to investigate the adsorption mechanism and other surface properties as adsorbent affinity. Sorption experiments were performed by batch method with 50 mg of the adsorbent material conducted with 5 ml metal ion solutions of La, Ce and Sm chlorides and Nd nitrate with concentration range 100–1000 mg l^{-1}. The pH of the prepared metal ion solutions were kept constant at the optimum neutral pH. The samples were established in thermostatic shaker water bath at desired reaction temperatures (25, 45 and 65 $\pm$ 1°C) until they reached the equilibrium time. The supernatant solution was analysed to determine the equilibrium metal ion concentration using UV-Visible spectrophotometer and the adsorption capacity was calculated from the following equation:

$$q_e = (c_0 - c_e)\frac{V}{m}\ \text{mg g}^{-1}, \tag{3}$$

where q_e is the amount of metal ion sorbed when equilibrium is attained (mg g^{-1}), C_0 and C_e are the initial and equilibrium concentrations (mg l^{-1}) of metal ion solution, V the volume of the solution (l), m the weight (g) of the adsorbent.

The most common models used for studying sorption isotherm are Langmuir, Freundlich, Dubinin–Radushkivech (D–R) and Temkin isotherm models. Langmuir model assumes that monolayer adsorptions occur at finite number of active sites, which are identical and equivalent (all sites have equal affinity for the adsorbate) with no transmigration of the adsorbate in the plane of the surface. Freundlich isotherm model is the earliest known relationship describing the non-ideal and reversible adsorption, not restricted to the formation of monolayer. This empirical model can be applied to multilayer adsorption, with non-uniform distribution of adsorption heat and affinities over the heterogeneous surface. D–R model was used to distinguish the physical and chemical adsorption of metal ions with its mean free energy, E, per molecule of adsorbate (for removing a molecule from its location in the sorption space to the infinity). Temkin model assumes that the heat of adsorption (function of temperature) of all molecules in the layer would decrease linearly with coverage. All molecules adsorbed into the adsorbent have a uniform distribution of binding energies.

3. Result and discussion

Various samples of new poly-o-toluidine-based organic–inorganic fibrous-type composite ion-exchange materials were developed by incorporating poly-o-toluidine into inorganic matrices of fibrous Zr(IV) tungstophosphate. Among them, sample S-17 (table 1) possessed good yield, better sodium ion-exchange capacity and both chemical and thermal stabilities. Also, sample S-17 of POTZr(IV)WP exhibited granulometric and mechanical properties, showing a good reproducible behaviour as is evident from the fact that these materials obtained from various batches did not show any appreciable deviation in their percentage of yield and ion-exchange capacities. It was also found that the values of H^+ adsorption and H^+ liberation capacities are in close agreement. This material possessed a better Na^+ exchange capacity (1.8 meq g^{-1}) as compared to Zr(IV) tungstate (0.38 meq g^{-1}) and Zr(IV) tungstophosphate (0.92 meq g^{-1}). So POTZr(IV)WP (S-17) is better than the existing ones.

The chemical stability of POTZr(IV)WP and Zr(IV)WP in the aggressive media is shown in figure 1a and b. From this figure, it can be seen that POTZr(IV)WP resins have good chemical stabilities in 0.1 to 4 M HCl and 0.1 to 4 M HNO_3 aqueous solutions. The chemical stability of POTZr(IV)WP in HNO_3 was better than in HCl. POTZr(IV)WP is fairly stable in CH_3COOH and NaOH media. The stability of POTZr(IV)WP was less than Zr(IV)WP in both of HCl and HNO_3. The chemical stability may be due to the presence of binding polymer, which can prevent the dissolution of heteropolyacid sols or leaching of any constituent element into the solution [14]. Chemical stability of this resin is much higher than that of the similar materials obtained on the base of POT resins. Thus, exchanger is chemically resistant to most of the solvents and can be successfully used with diverse solvents in column operation.

The pH titration curves for POTZr(IV)WP composite cation exchanger was obtained under equilibrium conditions

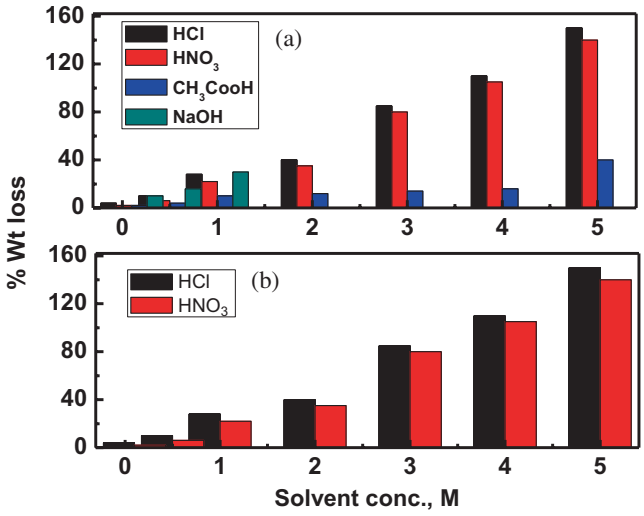

Figure 1. Chemical stability of (**a**) POTZr(IV)WP and (**b**) Zr(IV)WP in various solvents.

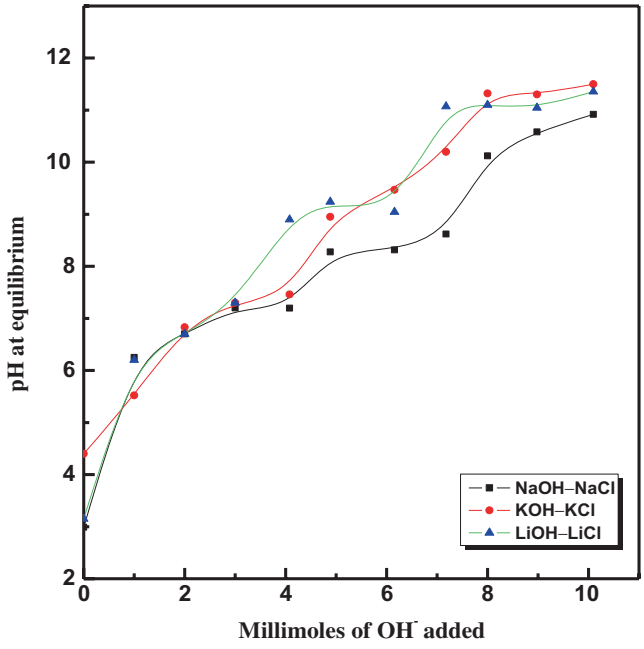

Figure 2. pH titration curve of LiCl–LiOH, NaCl–NaOH and KCl–KOH onto POTZr(IV)WP.

with solutions of NaCl–NaOH, LiCl–LiOH and KCl–KOH systems, which show two inflection points that indicate the bifunctional of the cation exchange behaviours (figure 2). The nano-composite materials appear to be a strong cation-exchanger as indicated by a low pH (∼3) of the solutions when no OH^- ions were added to the system, with further addition of OH^- ions to the metal chloride solution the pH increases rapidly, as H^+ liberated from the material and replaced with alkali ions until the solution was neutralized and acidic groups of hybrid cation exchanger are completely converted into the alkali form. This means that all H^+ ions on the hybrid cation-exchanger were exhausted and replaced

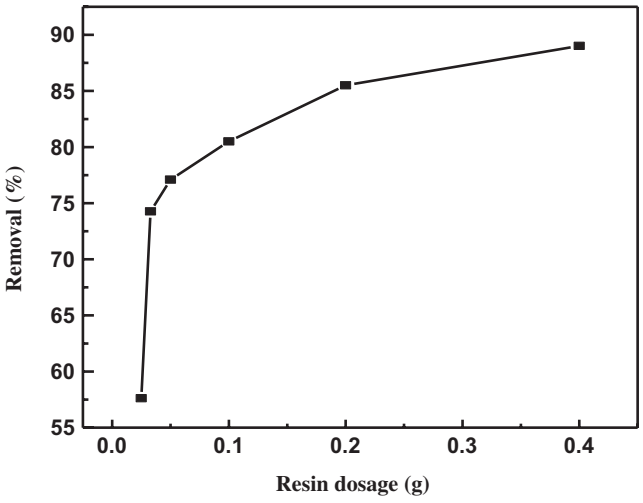

Figure 3. Effect of resin dosage on sorption of Sm(III) onto POTZr(IV)WP.

with alkali ions, and the numbers of H^+ liberated from the material were equivalent to the same amount of alkali interred. It is interesting to note that, H^+–Na^+ exchange was faster in comparison to H^+–Li^+ and H^+–K^+ exchanges, as evident from lower pH values in case of NaCl–NaOH system indicating higher release of H^+ ions [15]. Thus, the rate of exchange of H^+ in POTZr(IV)WP composite cation exchanger was found to be in order of $Na^+ > Li^+ > K^+$.

The effect of POTZr(IV)WP dosage on the percent removal of Sm(III) ion is presented in figure 3. It shows that the removal percent of Sm(III) ion increased from 57.6 to 89.02 with increase in the adsorbent mass from 0.025 to 0.4 g. This increase in the removal percent of metal ion was due to increase in the adsorbent mass; therefore, the surface area also increased indicating that more active sites are available for metal ion sorption process. It was concluded that the optimum $V/m = 100$, this percent was chosen as its removal percent is high and the resin mass is low (0.1 g) compared with $V/m = 25$, where its removal percent is slightly high and the resin mass used (0.4 g) was four times higher than the resin mass used to obtain $V/m = 100$.

Infrared spectroscopy is a valuable tool for providing structural information and identification of unknown compounds. It is used to investigate molecular systems containing various chromospheres. The FT-IR spectra of different prepared samples are shown in figures 4–6. The FT-IR spectrum of different samples indicates the presence of extra water molecule in addition to –OH groups and metal oxides present in the material. A strong and broad peak around 3400 cm^{-1} corresponds to the presence of interstitial water and hydroxyl groups [16]. A sharp peak at 1670 cm^{-1} corresponds to H–O–H bending band, being also representative of the strongly bonded –OH groups in the matrix [17]. Peaks observed at 2920–2847 cm^{-1} resulted from C–H and at 1378 cm^{-1} due to C–N stretching vibration band due to entering CTAB compound [18]. Spectrum also showed broad bands in the region 830–780 cm^{-1} and 951 cm^{-1} as in figure 4a

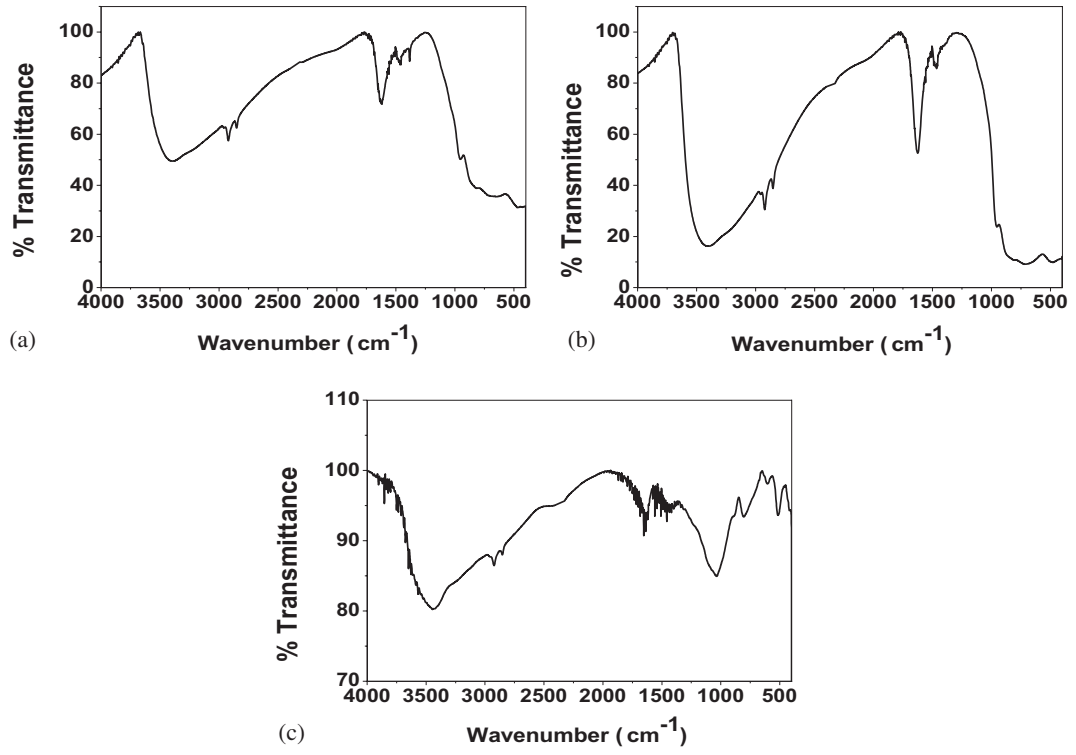

Figure 4. The IR spectra of (**a**) Zr(IV)W, (**b**) Zr(IV)W hydrothermal method and (**c**) Zr(IV)WP.

and b, which can be assigned to the presence of WO_4^{2-} and metal-oxide groups, respectively [19,20]. An assembly of three peaks in the 500–800 cm^{-1} region may be due to the presence of $PO4^{3-}$, HPO_4^{2-}, $H_2PO_4^{2-}$ as in figure 4c [21,22]. Peaks at 1478 cm^{-1} and 1127 are due to N–H bending vibration and C–C stretching vibration band, respectively, shown in figure 5(a–c). Peaks at 1378 and 1066 cm^{-1} are due to C–N and C–H stretching vibration band of in–plane, as in figure 5c. From the IR spectra of POTZr(IV)W prepared by different methods, POTZr(IV)W prepared by insitue method was the best according to the IR spectra, so was used for latest synthesis.

Figure 6a and b shows the FT-IR spectra for POT and POTZr(IV)WP, the band at 3423 cm^{-1} attributed to NH_2 asymmetric stretching vibrations. The band at 3220 cm^{-1} attributed to N–H stretching vibration, which suggests the presence of N–H groups in POT units as in figure 6a. The band at 2861 cm^{-1} is attributed to the C–H stretching vibration of methyl group of o-toluidine, as in figure 6a and b [23]. A stretching mode of N–H unsaturated amine is represented by a band at 2337 cm^{-1}. The skeletal vibrations of the aromatic rings show two bands at 1609 and 1481 cm^{-1}, which are assigned to C=C stretching vibrations of quinoid and benzoid rings, respectively, as in figure 6a and b. The FT-IR spectra show that the relative intensity of benzoid ring stretching at 1481 cm^{-1} is higher than that of quinoid ring stretching at 1609 cm^{-1}, as in figure 6a. This suggests the presence of a higher fraction of benzoid rings in the synthesized POT [24]. The band at 1323 cm^{-1} can be attributed to C–N stretching vibration of aromatic rings, indicating the presence of secondary aromatic amine groups, as in figure 6a and b [25]. The band at 1108 cm^{-1} attributes to C–H in-plane bending) and at 806 cm^{-1} attributes to C–H deformation in the methyl group attached to the phenyl ring [26]. The bands at 1029 cm^{-1} are due to in-plane C–H vibration (γ C–H). The bands at 806 and 617 cm^{-1} are assigned to an out-of-plane C–H vibration (γ C–H) for quinoid and benzoid rings, respectively. Figure 6b shows that the FT-IR spectra of POTZr(IV)WP composites are almost identical to that of POT, indicating that o-toluidine was polymerized on the surface of Zr(IV)WP to form POTZr(IV)WP composites [27].

TGA-DTA curves, figures 7 and 8, of POTZr(IV)WP and Zr(IV)WP, respectively, showed continuous mass weight loss, about 5.472% for POTZr(IV)WP and 10% for Zr(IV)WP, up to 200°C, which may be due to the removal of external water molecule that supported endothermic peak of DTA curve at 95°C for POTZr(IV)WP and 72°C for Zr(IV)WP [28]. A slow weight loss observed between 200 and 400°C may be due to the condensation of phosphate group to pyrophosphate groups supported by exothermic peak at 350°C for POTZr(IV)WP and Zr(IV)WP [29]. A high weight loss observed between 400 and 700°C may be due to decomposition of organic part of the material that corresponds to the endothermic peak at 650°C for POTZr(IV)WP. Above 700°C very slight (negligible) mass weight loss observed may be due to the formation of metal oxide forms of the material. The total mass weight loss was 29.357% up to 1000°C. Figure 5 shows TGA–DTA curve for Zr(IV)WP and the total weight loss was found to be 17.9% up to 800°C. The total

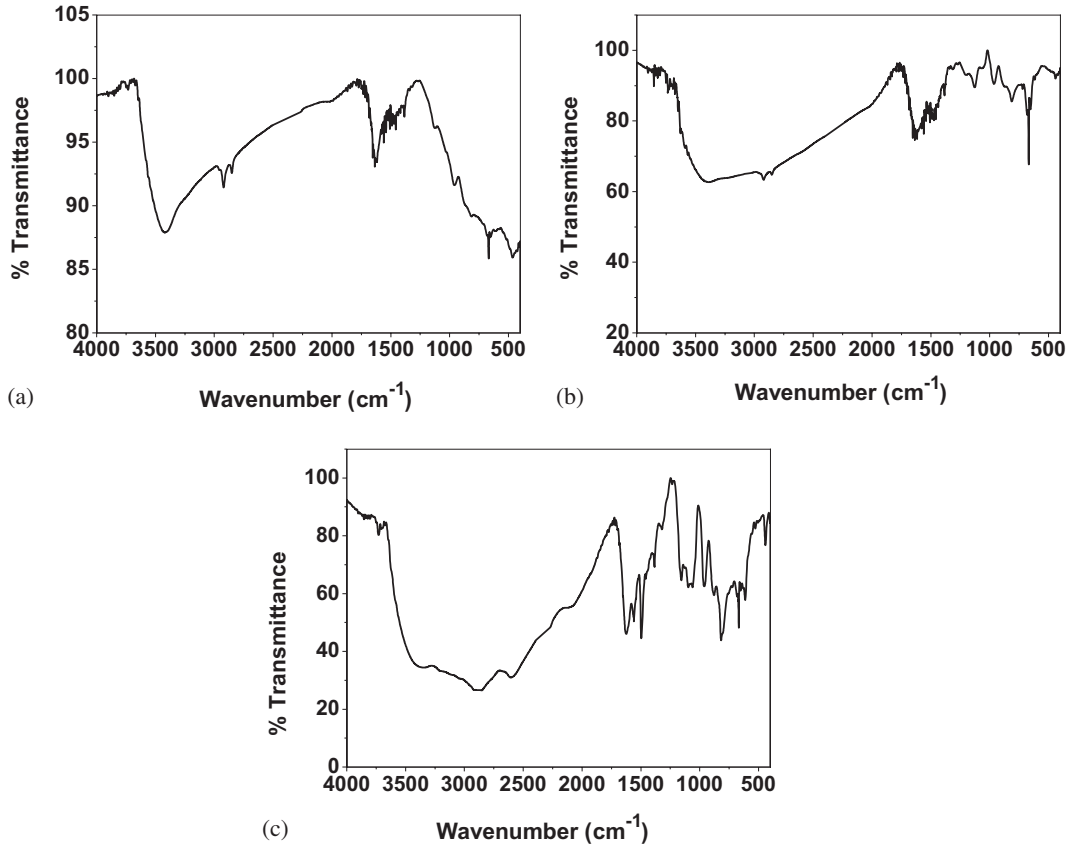

Figure 5. FT-IR spectra of POTZr(IV)W synthesized with (**a**) mixing, (**b**) insitue and (**c**) chelation methods.

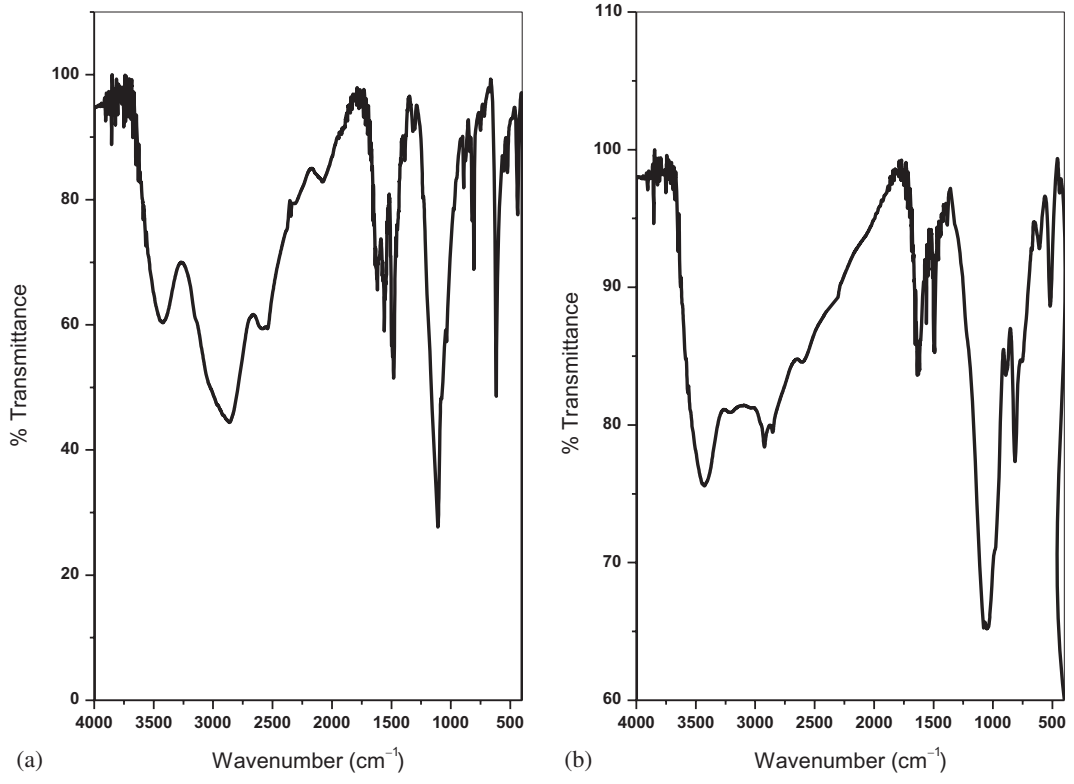

Figure 6. FT-IR spectra of (**a**) POT and (**b**) POTZr(IV)WP.

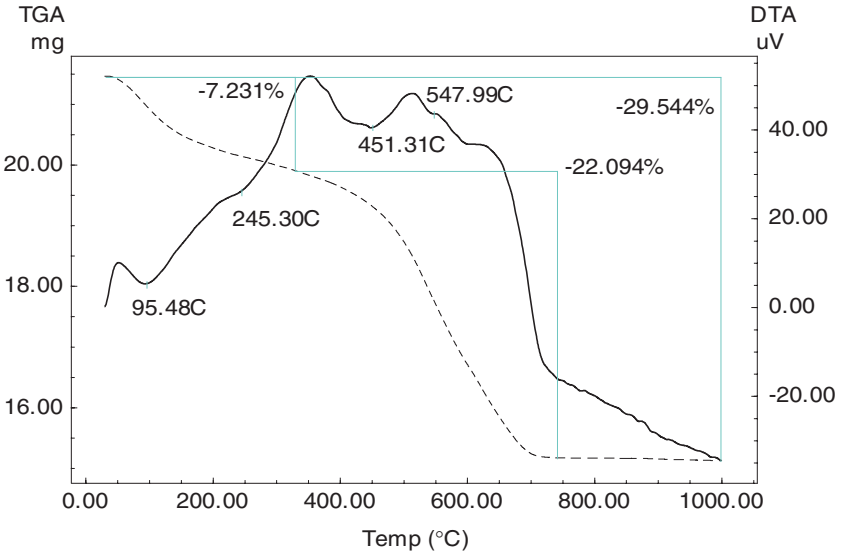

Figure 7. TGA–DTA of POTZr(IV)WP composite material.

weight loss of Zr(IV)WP was less than POTZr(IV)WP, as organic part in POTZr(IV)WP decomposed at 400°C.

From the elemental composition data and elemental analysis, the weight composition percent of the material was found to be Zr, 22.13%; W, 44.603%; P, 7.514%; C, 20.398%; H, 1.956% and N, 3.398%. The corresponding molar ratio of Zr, W, P, C, H and N was calculated as 1:1:1:7:9:1, which can suggest the following formula:

$$[ZrWO_4H_2PO_4{-}C_7H_7N{-})] \cdot nH_2O$$

and its structure unit can be written as:

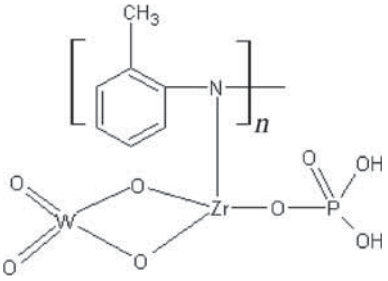

The mass weight loss was 5.47%, which was lost at 200°C represented by TGA curve due to the loss of nH_2O from the above structure. Alberti's equation was used to calculate the value of n as given below [30]:

$$18n = \frac{X(M + 18n)}{100}, \tag{4}$$

where X is the weight loss percent (5.472%) of the exchanger by heating up to 200°C and (M + 18n) is the molecular weight of the material. It was found that $n = 1.78$ per molecule of the cation exchanger and this crystalline water molecules can be used as active site for exchange process.

Figure 9 shows the XRD pattern of POTZr(IV)WP, indicating the semi-crystalline nature. The crystallite size, D, was estimated by calculating the broadening of the more intensity diffraction peak (strongest peak) according to Scherrer equation.

$$D = K\lambda/\beta\cos\theta, \tag{5}$$

where λ is the wavelength of incident X-ray of copper radiation source (0.154 ± 0.56 nm), K a constant depending on diffraction technique (here $K = 0.89$), β FWHM of Bragg peak observed at Bragg angle θ (in radian) and θ the angle of incidence of X-ray beam. It is obvious that the crystallite size of POTZr(IV)WP was 1.11 ± 0.02 nm.

In order to know the surface morphology of poly-o-toluidine, Zr(IV)WP and POTZr(IV)WP composite materials SEM was used. Figure 10a–c represent the SEM photographs of poly-o-toluidine and Zr(IV)WP and POTZr(IV)WP composite materials. The composite picture was different from that of poly-o-toluidine and Zr(IV)WP pictures. The difference in surface morphology may be related to the formation of POTZr(IV)WP composite by binding the polymer with Zr(IV)WP. According to figure 10c, it can be seen that POTZr(IV)WP was spherically shaped.

The adsorption isotherms can give the most important information about the distribution of the adsorbate molecules between the liquid and solid phases when the adsorption process reaches an equilibrium state. The surface properties and affinity of the adsorbent can be expressed by constant values of sorption isotherm models and can also be used to determine the adsorption capacities for metal ions. Various isotherm equations like those Langmuir, Freundlich, Dubinin–Radushkevich and Temkin were used to describe the equilibrium characteristics of adsorption of La^{3+}, Ce^{3+}, Nd^{3+} and Sm^{3+} ions onto POTZr(IV)WP. The accuracy of isotherm model usually related to the number of independent parameters on its equation and mathematical simplicity of any model makes it popular in the analysis of the obtained experimental data.

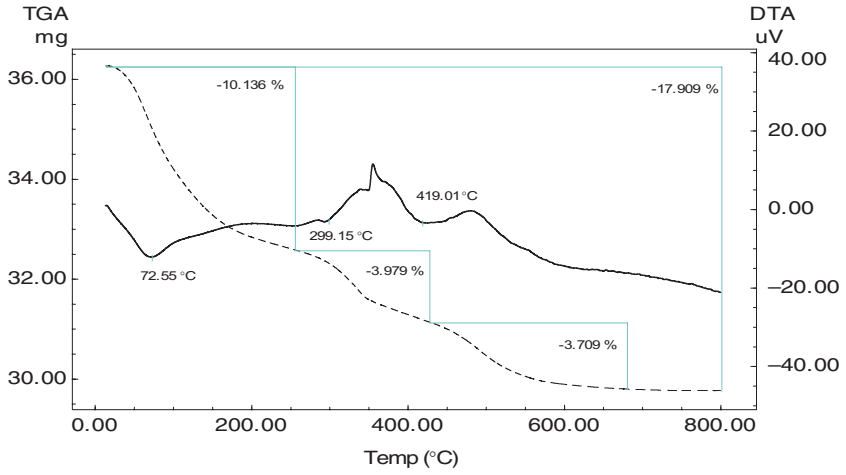

Figure 8. TGA–DTA of Zr(IV)WP inorganic adsorbent.

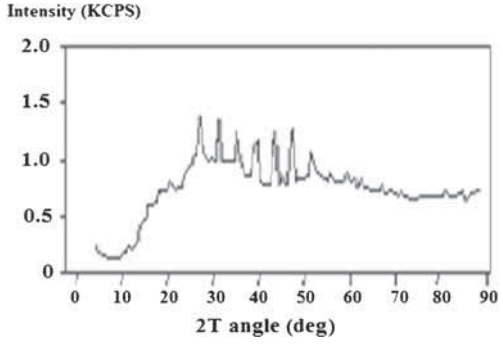

Figure 9. XRD pattern of POTZr(IV)WP composite cation exchanger.

In 1918, Langmuir has developed a theoretical equilibrium isotherm relating to the amount of gas adsorbed on a surface. Now, this model is a well-known isotherm model and widely used to quantify the performance of different adsorbents [31]. The Langmuir equation is applicable to homogeneous adsorption based on the following assumptions:

(1) Adsorption can only occur at a finite number of definite localized sites;
(2) All binding sites possess the same affinities for adsorption of a single molecular layer;
(3) There is no transmigration of the adsorbate on the plane of the surface;
(4) All sites are of equal size and shape on the surface of adsorbent.

The Langmuir equation is given as:

$$\frac{C_e}{q_e} = \frac{1}{bQ_o} + \frac{C_e}{Q_o}, \tag{6}$$

where Q_o is the maximum adsorption capacity (mg g^{-1}) and b the Langmuir constant (l mg^{-1}) related to the energy of adsorption which reflects the affinity between the adsorbent and adsorbate.

A plot C_e/q_e *vs.* C_e (figure 11) yields a straight line with slope $1/Q_o$ and intercepts $1/bQ_o$. The values of Langmuir equation parameters are given in table 2. The Langmuir model effectively and significantly described the sorption data with the R^2 values 0.992, 0.989, 0.996 and 0.99 for sorption of La^{3+}, Ce^{3+}, Nd^{3+} and Sm^{3+} onto POTZr(IV)WP at 25°C, respectively. According to the Q_m (mg g^{-1}) parameter, monolayer capacity at 25°C of POTZr(IV)WP was arranged in the following sequence, Sm > La > Nd > Ce. These metals seem to reach saturation, which means that the metal had clogged possible available sites in POTZr(IV)WP and further adsorption could take place only at new surfaces [32,33]. Also, from table 2 it is observed that an increase in the saturation capacity with increase of temperature reflects a better accessibility of the sorption sites. Based on K_L values increase in the sequence, Sm > La > Nd > Ce; samarium has higher affinity for POTZr(IV)WP, which is well correlated with the higher adsorption capacity Q_m obtained.

The essential characteristics and the feasibility of the Langmuir model were expressed by Weber and Chakravot in terms of a dimensionless constant, commonly known as separation factor (R_L), expressed by the following equation [34]:

$$R_L = \frac{1}{1 + bC_o}. \tag{7}$$

The R_L values indicate either the shape of adsorption isotherm is unfavourable ($R_L > 1$) or favourable ($0 < R_L < 1$) or linear ($R_L = 1$) or irreversible ($R_L = 0$).

Values of R_L calculated at 25, 35 and 40°C for all concentrations of studied ion solutions (table 2) were in the range between 0 and 1, which indicate that the adsorption process is favourable at operation conditions studied. For each ion, the R_L value decreases with the rise in temperature, suggesting an increase in the affinity between lanthanide ions and POTZr(IV)WP.

In 1906, Freundlich had proposed the earliest known sorption equation. It can be applied to non-ideal adsorption or

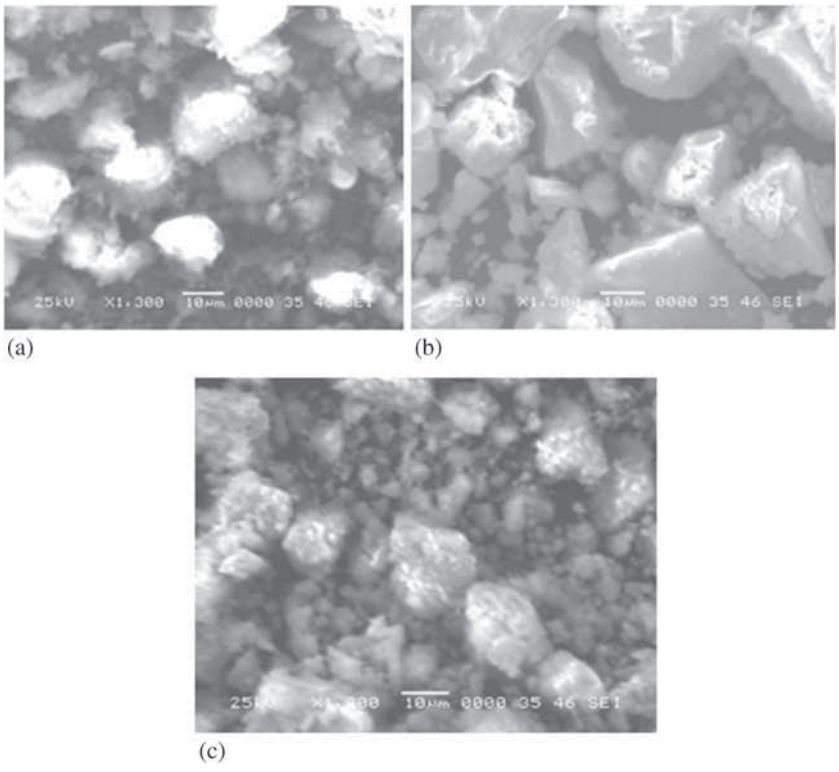

Figure 10. Scanning electron microphotograph of (**a**) poly-o-toluidine (POT), (**b**) Zr(IV)WP and (**c**) POTZr(IV)WP at magnification of 1,300.

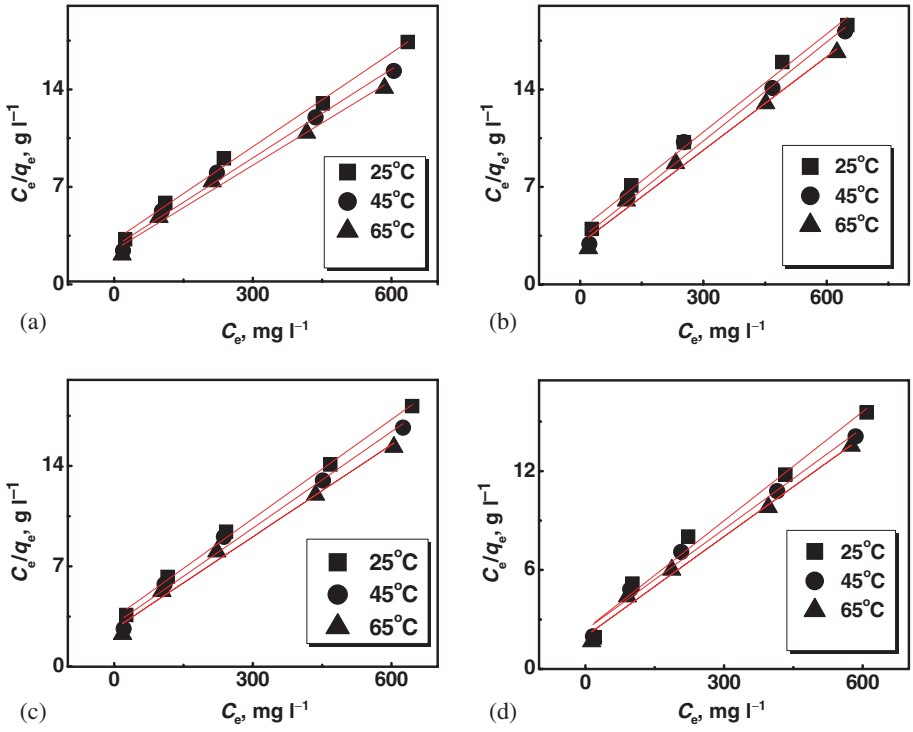

Figure 11. Langmuir isotherm model plots of (**a**) La^{3+}, (**b**) Ce^{3+}, (**c**) Nd^{3+} and (**d**) Sm^{3+} ion sorption onto POTZr(IV)WP at different temperatures.

Table 2. Langmuir, Freundlich, D–R and Temkin isotherm model parameters for sorption of La^{3+}, Ce^{3+}, Nd^{3+} and Sm^{3+} ion onto POTZr(IV)WP composite material at different reaction temperatures.

	Lanthanum			Cerium			Neodymium			Samarium		
Isotherm models	25°C	45°C	65°C	25°C	45°C	65°C	25°C	45°C	65°C	25°C	45°C	65°C
Langmuir parameters												
Q_o (mg g^{-1})	44.54	47.01	49.33	42.61	42.33	44.72	43.38	44.66	46.68	46.93	48.99	49.58
b ($\times 10^{-3}$ l mg^{-1})	7.12	7.8	8.20	6.0	7.33	7.62	6.77	7.59	8.13	7.86	8.65	10.21
R_L	0.58	0.56	0.54	0.62	0.57	0.56	0.59	0.56	0.55	0.56	0.53	0.49
R^2	0.992	0.987	0.984	0.989	0.982	0.985	0.996	0.984	0.985	0.990	0.985	0.988
Freundlich parameters												
$1/n$	0.493	0.469	0.468	0.504	0.459	0.463	0.498	0.464	0.459	0.477	0.458	0.447
K_F ($mg^{(1-1/n)}$ $l^{1/n}$ g^{-1})	1.68	2.09	2.25	1.41	1.94	2.03	1.55	2.02	2.22	1.99	2.39	2.72
R^2	0.976	0.989	0.991	0.981	0.989	0.991	0.974	0.99	0.991	0.983	0.991	0.983
D–R parameters												
Q_m ($\times 10^{-4}$ mol g^{-1})	7.77	7.68	8.02	7.28	6.61	7.07	7.22	7.42	6.94	7.45	7.38	7.53
K ($\times 10^{-3}$ mol^2 k^{-1} J^{-2})	5.73	4.69	4.00	5.94	4.65	4.09	4.00	5.82	4.62	4.62	4.46	3.79
R^2	0.993	0.992	0.999	0.995	0.997	0.998	0.999	0.992	0.999	0.997	0.998	0.993
E (kJ^{-1} mol^{-1})	9.33	10.31	11.04	9.17	10.36	11.04	11.17	9.26	10.39	9.61	10.57	11.47
Temkin parameters												
$b \times 10^{-5}$ (kJ mol^{-1})	6.59	6.66	6.91	6.25	5.96	6.27	6.23	6.10	6.30	6.25	6.29	6.33
$A \times 10^3$ (l g^{-1})	11.64	13.98	14.26	9.89	1.20	1.43	11.04	13.46	16.03	14.76	18.20	21.00
R^2	0.984	0.975	0.969	0.984	0.971	0.970	0.990	0.970	0.970	0.980	0.967	0.965

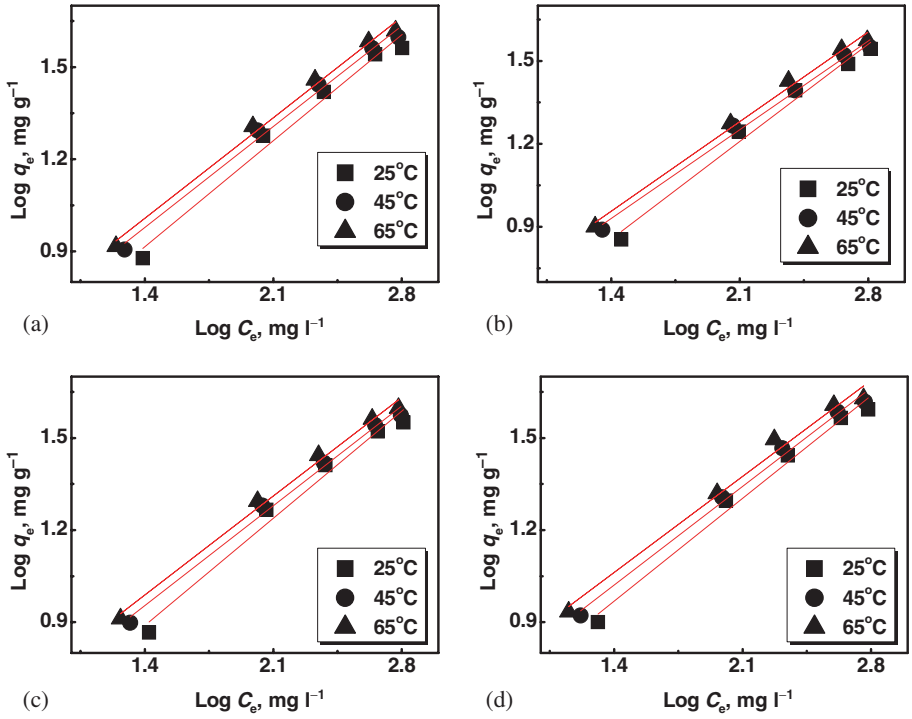

Figure 12. Freundlich isotherm model plots of (**a**) La^{3+}, (**b**) Ce^{3+}, (**c**) Nd^{3+} and (**d**) Sm^{3+} ion sorption onto POTZr(IV)WP at different temperatures.

multilayer sorption of adsorbate on heterogeneous surface based on the following assumptions: (1) the heat of adsorption decrease with increase in surface coverage of adsorbent and (2) the adsorption sites on the surface of adsorbent have different adsorption energies.

At present, Freundlich isotherm is widely used in different heterogeneous systems [35] and is expressed by the following equation:

$$\log q_e = \log K_F + \frac{1}{n} \log C_e, \tag{8}$$

where q_e is the adsorbed amount of metal ion (mg g^{-1}), C_e is the equilibrium concentration of metal ion (mg l^{-1}), K_F represents the adsorption capacity for a unit equilibrium concentration, while $1/n$ is the indicative of the energy or intensity of the reaction and suggests the favourability and capacity of the adsorbent–adsorbate system. The values of Freundlich isotherm constants (K_F and $1/n$) determined from the linear plot of log q_e *vs.* log C_e, as in figure 12, are presented in table 2.

Similarly to R_L values from Langmuir isotherm, the $1/n$ value indicates the type of isotherm as follows: irreversible ($1/n = 0$), favourable ($0 < 1/n < 1$), or unfavourable ($1/n > 1$). The Freundlich constants, $1/n$, shown in table 2 indicate that La^{3+}, Ce^{3+}, Nd^{3+} and Sm^{3+} ions were adsorbed favourably by POTZr(IV)WP at all the different temperatures. The adsorption capacity (K_F) at 25°C of POTZr(IV)WP was arranged in the following sequence, Sm > La > Nd > Ce and is observed that its value increases with the increase in temperature. This sequence agreement with monolayer capacity Q_m was calculated from Langmuir isotherm. The R^2 values were 0.976, 0.981, 0.974 and 0.983 for sorption of La^{3+}, Ce^{3+}, Nd^{3+} and Sm^{3+} onto POTZr(IV)WP at 25°C, respectively. The R^2 Langmuir values are higher than Freundlich values. It can be seen that a good fitting of Langmuir model to experimental data is achieved. Similar behaviour was observed in adsorption process of Cs^+ on polyaniline titanotungstate composite cation exchanger [36].

Another equation used in the analysis of adsorption isotherms was proposed by Dubinin and Radushkevich [37]. This model was used to estimate the apparent free energy of adsorption as well as to make a difference between physical and chemical adsorption process. The D–R equation was given by the following relationship:

$$\ln q_e = \ln Q_m - K\varepsilon^2, \tag{9}$$

where Q_m is the theoretical saturation capacity, K the activity coefficient related to mean sorption energy and ε the polanyi potential given by:

$$\varepsilon = R_g T \ln\left(1 + \frac{1}{C_e}\right), \tag{10}$$

where R is the gas constant (8.314 kJ mol^{-1} K^{-1}) and T the temperature (K).

The values of isotherm constants (Q_m and K) obtained by plotting ln q_e *vs.* ε^2, as in figure 13, are given in table 2. The D–R constant can give the valuable information regarding the mean energy of adsorption by the following equation:

$$E = (-2K)^{-0.5}. \tag{11}$$

It is known that the magnitude of E gives the information about the type of adsorption process: physical (1–8 kJ mol^{-1}), ion exchange (9–16 kJ mol^{-1}) and chemical (>16 kJ mol^{-1}) [38]. The apparent free energies of La^{3+}, Ce^{3+}, Nd^{3+} and Sm^{3+} adsorption on POTZr(IV)WP at different temperatures were calculated to be in the range of 9.26–11.47 kJ mol^{-1}, which means that the process is ion exchange adsorption.

Temkin and Pyzhev isotherm was proposed to describe for the first time the adsorption of hydrogen onto platinum electrodes within the acidic solution [39]. The assumptions made

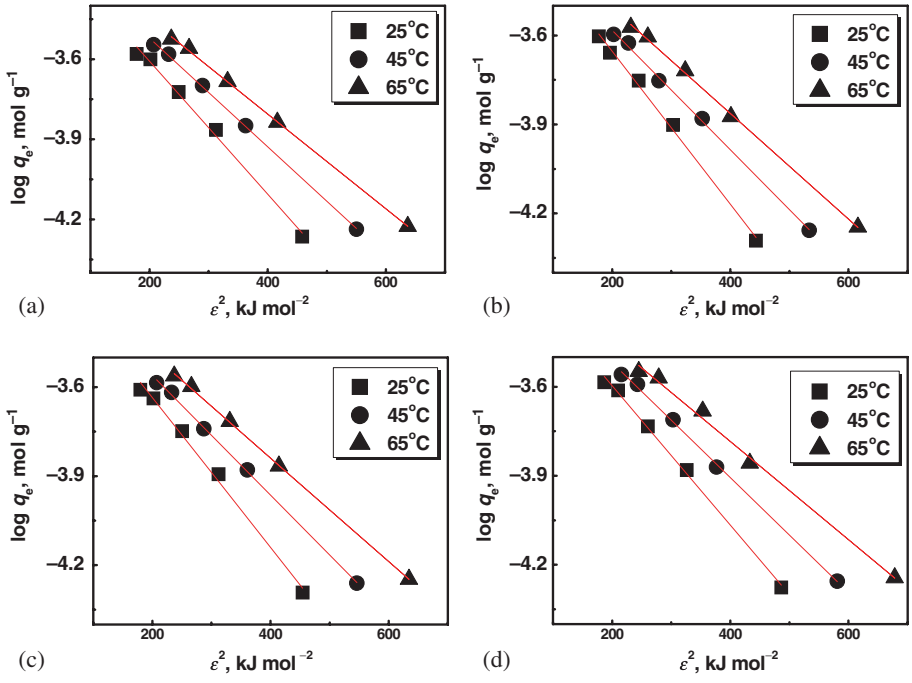

Figure 13. D–R isotherm model plots of (**a**) La^{3+}, (**b**) Ce^{3+}, (**c**) Nd^{3+} and (**d**) Sm^{3+} ion sorption onto POTZr(IV)WP at different temperatures.

on the Temkin adsorption model are that: (a) adsorption is characterized by a uniform distribution of binding energies; (b) the heat of adsorption of all the molecules in the layer would decrease linearly with coverage due to adsorbent–adsorbate interactions. The linear form of Temkin isotherm is given below:

$$q_e = b \ln A + b \ln C_e, \tag{12}$$

where b is the Temkin constant related to the heat of adsorption (J mol^{-1}) and A the equilibrium binding constant corresponding to the maximum binding energy (l mg^{-1}).

By plotting q_e against ln C_e, as in figure 14, we can obtain Temkin constants A and b as intercept and slope. The values of the Temkin parameters are given in table 3. The Temkin constant b for the adsorption of La^{3+}, Ce^{3+}, Nd^{3+} and Sm^{3+} on POTZr(IV)WP was $\leq 6.91 \times 10^{-5}$ kJ mol^{-1} at different temperatures. The low value of b confirmed that the interaction between metal ions and the POTZr(IV)WP surface was week and ion exchange was the most suggested mechanism [40]. Based on correlation coefficient shown in table 2, the results indicate that the Langmuir and Dubinin–Radushkevich models represent a better fit of experimental data than Freundlich and Temkin models.

The sorption amounts of single metal ions by POTZr(IV)WP are measured at temperature range 298–338 K. The thermodynamic parameters including Gibbs free energy (ΔG^o), enthalpy (ΔH^o) and entropy changes (ΔS^o) can be calculated using the following equations [41]:

$$\Delta G^o = -RT \ln K_c, \tag{13}$$

where R is the universal gas constant (8.314 J mol^{-1} K^{-1}), T the temperature (K) and K_c the equilibrium constant. The K_c value was calculated using the following equation:

$$K_c = q_e / C_e, \tag{14}$$

where q_e (mg l^{-1}) and C_e (mg l^{-1}) are the equilibrium concentration of metal ions adsorbed onto POTZr(IV)WP and remained in the solution, respectively. The enthalpy (ΔH^o)

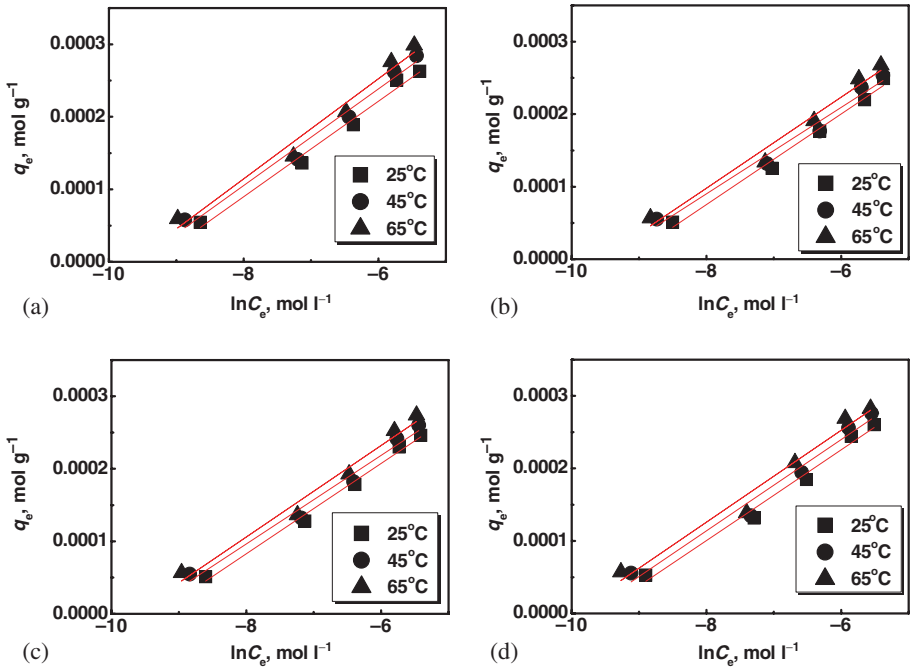

Figure 14. Temkin isotherm model plots of (**a**) La^{3+}, (**b**) Ce^{3+}, (**c**) Nd^{3+} and (**d**) Sm^{3+} ion sorption onto POTZr(IV)WP at different temperatures.

Table 3. Thermodynamic parameters of La^{3+}, Ce^{3+}, Nd^{3+} and Sm^{3+} ion sorbed onto POTZr(IV)WP.

	ΔG° (kJ mol^{-1})$^{-1}$					
Metal ion	25°C	45°C	65°C	ΔH^o (kJ mol^{-1})$\times 10^{-3}$	ΔS^o (J mol^{-1} K^{-1})	R^2
La^{3+}	–2.78	–3.74	–4.35	8.95	39.59	0.937
Ce^{3+}	–2.27	–3.26	–3.81	9.19	38.71	0.904
Nd^{3+}	–2.52	–3.51	–4.16	9.72	41.34	0.949
Sm^{3+}	–3.35	–4.28	–4.94	9.31	42.59	0.987

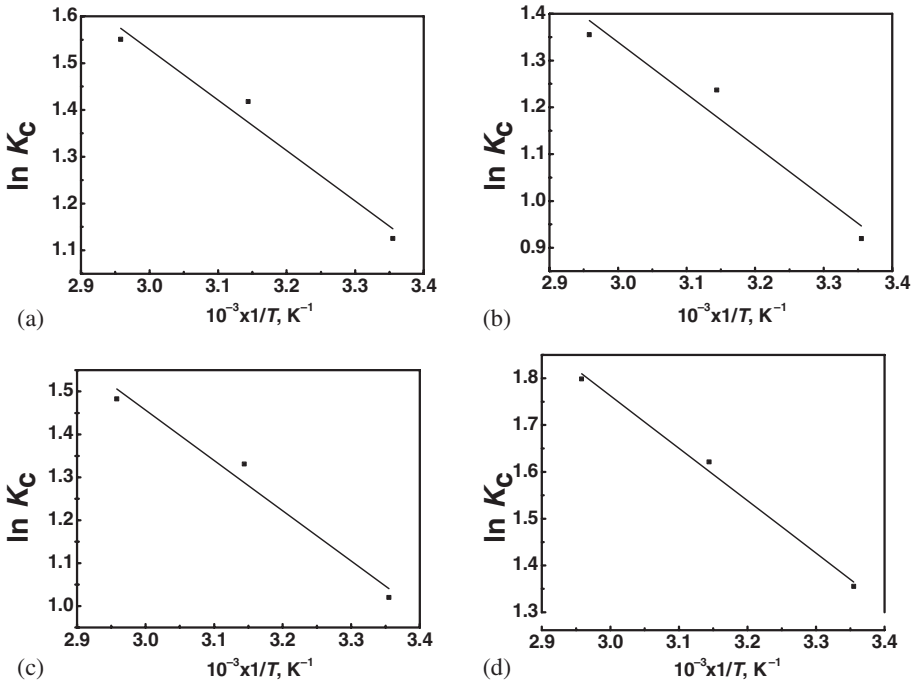

Figure 15. Plots of ln K_c *vs.* $1/T$ for the sorption processes of (**a**) La^{3+}, (**b**) Ce^{3+}, (**c**) Nd^{3+} and (**d**) Sm^{3+} ion onto POTZr(IV)WP.

and entropy (ΔS^o) changes of adsorption were estimated from the following equation:

$$\Delta G^o = \Delta H^o - T\Delta S^o. \tag{15}$$

This equation can be written as

$$\ln K_c = \frac{\Delta S^o}{R} - \frac{\Delta H^o}{RT}. \tag{16}$$

According to Equation (16), the ΔH^o and ΔS^o were calculated from the slope and intercept of the plot between ln K_d *vs.* $1/T$, respectively, as in figure 15 and table 3. All these relations are valid when the enthalpy change remains constant in the temperature range. The ΔG^o values were obtained by using Equation (13) in the temperatures of 25, 45 and 65°C. The negative values of ΔG^o, for La^{3+}, Ce^{3+}, Nd^{3+} and Sm^{3+} ions, suggested the feasibility of the present adsorption process and spontaneous nature of the adsorption of La^{3+}, $Ce^{3+,}$ Nd^{3+} and Sm^{3+} ions onto POTZr(IV)WP (table 3). On the other hand, the magnitude of ΔG^o increased with increase in the temperature, indicating that a better adsorption is actually obtained at higher temperatures. The positive values of ΔH^o, for these ions, indicated that the endothermic nature of adsorption process was also supported by the increase in amount of metal uptake with the rise in temperature. One possible explanation of endothermic of heats of adsorption maybe due to the sorption process of metal ions onto adsorbent material requires at first solvation of these ions. For the metal ions to be adsorbed, they have to lose part of their hydration sheath and dehydration process of ions required energy so the water removing process from ions is endothermic process [42]. The positive ΔS^o values suggested an increase in the randomness at the solid/solution interface during the adsorption of La^{3+}, Ce^{3+} Nd^{3+} and Sm^{3+} onto POTZr(IV)WP [43].

4. Conclusion

The FT-IR spectra of POTZr(IV)WP composites show that OT was polymerized on the surface of Zr(IV)WP to form POTZr(IV)WP composites. POTZr(IV)WP prepared by insitue method was the best according to the IR spectra. POTZr(IV)WP was stable in different media and at higher temperatures. XRD pattern shows that POTZr(IV)WP was in semi-crystalline nature. The formula of POTZr(IV)WP was found as $[(ZrO_2)(WO_2)(PO_4)(-C_7H_{11}N-)]\cdot 1.78H_2O$. The saturation capacity for the sorption of La^{3+}, Ce^{3+}, Nd^{3+} and Sm^{3+} was increased in the sequence Sm > La > Nd > Ce; where samarium has higher affinity for POTZr(IV)WP. The apparent free energies of La^{3+}, Ce^{3+}, Nd^{3+} and Sm^{3+} adsorption on POTZr(IV)WP at different temperatures were calculated to be in the range of 9.26–11.47 kJ mol^{-1}, which means that the process is ion exchange adsorption. The Temkin constant b for the adsorption of La^{3+}, Ce^{3+}, Nd^{3+} and Sm^{3+} on POTZr(IV)WP was $\leq 6.91 \times 10^{-5}$ kJ mol^{-1} at different temperatures. The low value of b confirmed that the interaction between metal ions and the POTZr(IV)WP surface was weak and ion exchange was the most suggested mechanism. Correlation coefficient indicates that the Langmuir and Dubinin–Radushkevich models represent a better fit of experimental data than Freundlich and Temkin models. The negative values of ΔG^o, for La^{3+}, Ce^{3+}, Nd^{3+}

and Sm^{3+} ions, suggested the feasibility of the present adsorption process and spontaneous nature of the adsorption onto POTZr(IV)WP. The positive values of ΔH^{o}, for La^{3+}, Ce^{3+}, Nd^{3+} and Sm^{3+} ions, indicated that the endothermic nature of adsorption process was also supported by the increase in amount of metal uptake with the rise in temperature. The positive ΔS^{o} values suggested an increase in the randomness at the solid/solution interface during the adsorption of La^{3+}, Ce^{3+}, Nd^{3+} and Sm^{3+} onto POTZr(IV)WP.

References

[1] Veliscek-Carolan J, Hanley T L and Luca V 2014 *Sep. Purif. Technol.* **129** 150

[2] Justyna J, Dorota K, Hubicki and Zbigniew 2010 *Can. J. Chem.* **88** 540

[3] Demirbas A, Pehlivan E, Gode F, Altun T and Arslan G 2005 *J. Colloid. Interf. Sci.* **282** 20

[4] Siddiqui W A, Khana S A and Inamuddin 2007 *J. Colloid. Surf. A* **295** 193

[5] El-Naggar I, Zakaria E and Ali I 2004 *Sep. Purif. Technol.* **39** 4

[6] Ali I, Zakaria E and El-Naggar I 2004 *Arab. J. Nucl. Sci. Technol.* **37** 31

[7] Zakaria E, Ali I and Aly H 2004 *Adsorption* **10** 45

[8] Varshney K G, Rafiquee M Z A and Somya A 2008 *Colloid. Surf. A* **317** 400

[9] El-Naggar I M, Zakaria E S, Ali I M, Khalil M and El-Shahat M F 2012 *Arab. J. Chem.* **5** 109

[10] El-Naggar I M, Zakaria E S, Ali I M, Khalil M and El-Shahat M F 2012 *J. Environ. Radioactiv.* **112** 108

[11] El-Naggar I M, Zakaria E S, Ali I M, Khalil M and El-Shahat M F 2012 *Adv. Chem. Eng. Sci.* **2** 166

[12] Topp N E and Pepper K W 1949 *J. Chem. Soc.* **3299**

[13] Abd El-Latif M M and Elkady M F 2011 *Desalination* **271** 41

[14] Khan A A and Inamuddin 2006 *React. Funct. Polym.* **66** 1649

[15] Nabi S A, Akhtar A, Khan Md D A and Khan M A 2014 *Desalination* **340** 73

[16] Ali I 2004 *J. Radioanal. Nucl. Chem.* **260** 149

[17] Rao C N R 1963 *Chemical applications of infrared spectroscopy* (NY: Academic Press) p 355

[18] Rao C N R 1963 *Chemical applications of infrared spectroscopy* (NY: Academic Press) p 250

[19] Davis M 1963 *Infrared spectroscopy and molecular structure* (Amsterdam: Elsevier Publishing Co.) p 318

[20] Miller F A and Wilkins C H 1952 *Anal. Chem.* **24** 1253

[21] Rao C N R 1963 *Chemical applications of infrared spectroscopy* (NY: Academic Press) p 353

[22] Khan A A and Akhtar T 2009 *Electrochimica Acta* **54** 3320

[23] Chabukswar V S, Bhavsar and Horne A 2011 *Chem. Technol.* **5** 37

[24] Kulkarni M V and Viswanath A K 2004 *Eur. Polym. J.* **40** 379

[25] Abdiryim T, Xiao-Gang Z and Jamal R 2005 *J. Appl. Polym. Sci.* **96** 1630

[26] Kulkarni M V, Viswanath A K and Mulik U P 2005 *Mater. Chem. Phys.* **89** 1

[27] Fujita I, Ishiguchi M, Shiota H, Danj T and Kosai K 1992 *J. Appl. Polym. Sci.* **44** 987

[28] Ali I M, Kotp Y H and Elnaggar I M 2010 *Desalination* **259** 228

[29] Khan A A, Inamuddin and Alam M M 2005 *Mater. Res. Bull.* **40** 289

[30] Alberti G, Torracca E and Conte A 1966 *J. Inorg. Nucl. Chem.* **28** 607

[31] Vasiliu S, Bunia I, Racovita S and Neagu V 2011 *Carbohyd. Polym.* **85** 376

[32] Ibrahim H S, Jamil T S and Hegazy E Z 2010 *J. Hazard. Mater.* **182** 842

[33] Ali I M, Zakaria E S, Ibrahim M M and El-Naggar I M 2008 *Polyhedron* **27** 429

[34] Weber T W and Chakravot R K 1974 *AIChE J.* **20** 228

[35] Freundlich H M F 1906 *Z. Phys. Chem.* **57** 385

[36] Khalil M, *Chemical studies on poly aniline titanotungstate as a new composite cation exchanger and its analytical applications for removal of cesium from aqueous solution*, Ain Shams University, Cairo, Egypt 2012

[37] Dubinin M M, Zaverina E D and Radushkevich L I V 1947 *Russ. J. Phys. Chem. A* **21** 1351

[38] Chabani M, Amrane A and Bensmaili A 2006 *Chem. Eng. J.* **125** 111

[39] Temkin M I and Pyzhev V 1940 *Acta Phys.-Chim. USSR* **12** 327

[40] Sheha R R and Metwally E 2007 *J. Hazard. Mater.* **143** 354

[41] Smith J M and Van Ness H C 1987 *Introduction to chemical engineering thermodynamics,* 4th edn (Singapore: McGraw-Hill)

[42] Zakaria E S, Ali I M and El-Naggar I M 2002 *Colloid. Surf. A* **210** 33

[43] Zakaria E S, Ali I M and Aly H F 2009 *J. Colloid. Interf. Sci.* **338** 346